Automated convective and stratiform precipitation estimation in a small mountainous catchment using X-band radar data in Central Spain

Carolina Guardiola-Albert, Carlos Rivero-Honegger, Robert Monjo, Andrés Díez-Herrero, Carlos Yagüe, Jose María Bodoque and Francisco J. Tapiador

ABSTRACT

For the purposes of weather nowcasting, flood risk monitoring and water resources assessment, it is often difficult to achieve a reliable spatio-temporal representation of rainfall due to a low rain gauge network density. However, quantitative precipitation estimation (QPE) has acquired new prospects with the introduction of weather radars, thanks to their higher spatio-temporal resolution. Although a wide number of QPE algorithms are available for using C-band radar data, only a few studies have employed X-band radar. In this study the microscale rainfall variability in a small catchment is automatically measured using short-range X-band radar variograms and classifying precipitation into convective and stratiform types with a recently published index. The aim is to apply a straightforward geostatistical algorithm, named ordinary kriging of radar errors (OKRE), to integrate X-band radar and rain gauge measurements in a mountainous catchment (15 km^2) in central Spain. As expected, convective events presented higher estimation errors due to their complex spatial and temporal variability. Despite this fact, errors are sufficiently small and results are reliable rainfall estimations. The two main contributions of this work are the adaptation of the OKRE method to small spatial scales and its application automatically differentiating between convective and stratiform events.

Key words | convective event, kriging, mountainous basin, quantitative precipitation estimation, stratiform event, X-band radar

Carolina Guardiola-Albert (corresponding author)
Andrés Díez-Herrero
Geological Survey of Spain,
C/Ríos Rosas 23,
Madrid 28003,
Spain
E-mail: *c.guardiola@igme.es*

Carlos Rivero-Honegger
Carlos Yagüe
Dept. Geofísica y Meteorología,
Universidad Complutense de Madrid,
Madrid 28040,
Spain

Robert Monjo
Climate Research Foundation (FIC),
C/ Gran Vía 22 (dupl.), 7°,
Madrid 28013,
Spain

Jose María Bodoque
Department of Geological and Mining Engineering,
University of Castilla-La Mancha (UCLM),
Toledo,
Spain

Francisco J. Tapiador
Institute of Environmental Sciences (ICAM),
University of Castilla-La Mancha (UCLM),
Toledo,
Spain

INTRODUCTION

High spatio-temporal resolution quantitative precipitation estimation (QPE) is an increasing requirement for many applications (e.g. weather forecasting, water resources assessment, flood risk management), and is especially important for hydrological modeling of floods during extreme events, allowing the uncertainty reduction of the inputs in the precipitation-runoff models and runoff forecasts (Zoccatelli *et al.* 2010; Gourley *et al.* 2011; Krajewski *et al.* 2011; Zhang *et al.* 2011; Lee *et al.* 2014). For most applications, the real-time estimation requirement adds a significant challenge to the interpolation procedure, as this should then be both automatic and efficient, providing robust interpolation of gauged data.

Traditionally, rain has been measured at ground level using rain gauges which record precipitation intensity (R); however, with them spatial representation is often low due to their sparse density (Villarini *et al.* 2008). Moreover, geostatistical interpolation methods (Creutin & Obled 1982; Grimes *et al.* 1999; Goovaerts 2000; Kyriakidis *et al.* 2001; Lloyd 2005; Carrera-Hernandez & Gaskin 2007; Chappell

doi: 10.2166/hydro.2016.225

et al. 2013; Berndt et al. 2014; Jewell & Gaussiat 2015; Nanding et al. 2015; Rabiei & Haberlandt 2015) such as univariate (e.g. ordinary kriging) and multivariate (e.g. kriging with external drift (KED) or co-kriging) require a minimum of 50–100 data points to ensure an appropriate geostatistical analysis (Journel & Huijbregts 1978; Webster & Oliver 1993). This implies an unrealistic rain gauge density for very small catchments, impossible to attain even in developed countries.

Developed from the 1940s onwards, weather radars have been increasingly used for QPE in hydrological modeling due to their high spatial resolution, real-time availability (Cole & Moore 2008; Ehret et al. 2008) and also a higher coverage than ground observations (e.g. over the sea). In contrast to rain gauges, weather radars do not provide a direct measure of rain, but record the reflectivity (Z) of particles at a certain height above the ground (Rogers & Yau 1989). A weather radar has the capacity to sweep the entire study area at a high time resolution a few minutes for S- and C-band radars (Rogers & Yau 1989; Fabry 2015), or even less than a minute for some X-band radars. Still the data it yields are subject to various errors that require correction (Hong & Gourley 2015). Marshall & Palmer (1948) related drop-size distribution to R, giving a power law of the reflectivity-to-rainfall relationship (or Z-R equation).

Z-R coefficients may vary depending on the origin of rainfall, the region, temperature, radar features, etc. For a further discussion on the power law relationship between Z and R, and the corresponding values of a and b coefficients for different kind of precipitations, Chapter 9 of Fabry (2015) can be consulted. All these variations prevent the direct use of radar rainfall fields obtained from classical Z-R equations, even with adjusted coefficients (Borga 2002). Therefore, sophisticated merging methods combining rainfall, radar and other available short time step data are required. Among the high number of radar-gauge merging techniques, geostatistical estimators in particular have been subject to intense development (Krajewski 1987; Creutin et al. 1988; Seo et al. 1990; Seo 1998; Sinclair & Pegram 2005; Schuurmans et al. 2007; Ehret et al. 2008; Velasco-Forero et al. 2009; Heistermann & Kneis 2011; Verworn & Haberlandt 2011, among others). Even within the area of geostatistical methods, there is a wide range of algorithms with varying degrees of complexity and success (e.g. KED or co-kriging). The method named ordinary kriging of radar errors (OKRE) by Erdin (2013) is similar to the combination approach suggested by Sinclair & Pegram (2005), known as conditional merging (MERG). Several authors have found that these methods outperform other geostatistical algorithms such as KED (Erdin 2013; Legorgeu 2013; Berndt et al. 2014), or perform very slightly worse (Goudenhoofdt & Delobbe 2009).

Small-scale rainfall variability should be taken into account to improve rainfall data resolution. Both QPE uncertainty and variability will affect the confidence of hydrological model predictions. All the references mentioned above used a C-band radar resolution of ~1 km, rendering it difficult to capture precipitation microscale variability, particularly strong in convective events (Sideris et al. 2014). Three of these studies were devoted to very small mountainous catchments, with quick rainfall-runoff response. Ehret et al. (2008) merged a C-band radar and gauge data in a 75 km^2 catchment with a resolution of 500 m, preserving both the relatively reliable rain gauge data and the accuracy concerning spatial variability of the radar image. Meanwhile, Germann et al. (2009) conducted a hydrological experiment analyzing C-band radar data with a resolution of 1 km in a small, steep catchment of 44 km^2. They found that radar estimations yielded overestimations compared with rain gauge measurements for convective situations with strong spatial rainfall variability. Heistermann & Kneis (2011) benchmarked six different QPE methods in two small mountainous basins of 15 and 49 km^2. They used one C-band radar with spatial resolution of 1 km and 16 rain gauges situated close by the study area, but only one of them is located inside one runoff gauge subbasin. They found that the merging method used by Ehret et al. (2008) performs the best according to cross validation and hydrological verification based on runoff simulation.

X-band radar measurements can have a resolution of 100 to some meters (Rico-Ramirez et al. 2007), registering small-scale precipitation heterogeneities (Anagnostou et al. 2010). Thus, X-band radar is ideally suited for local rainfall estimation (Delrieu et al. 1997; Gires et al. 2012), as illustrated in the PhD dissertation of Legorgeu (2013), who applied geostatistical techniques in an area of 1,300 km^2. Furthermore, for stream flow simulation purposes Shrestha et al. (2013) found X-band weather radar based estimations

of precipitation to be more accurate than estimates using C-band radar.

The objective of the present study is to obtain a reliable spatial and temporal distribution of precipitation intensity for a small mountainous catchment. Geostatistical interpolation is used to merge measurements in rain gauges and X-band radar data. Analysis of the results is performed distinguishing between stratiform and convective rainfall.

METHODOLOGY

Data preprocessing

A maximum time scale of 1 hour is required to capture time variability of fast rainfall events (Sideris *et al.* 2014). Smaller accumulation time periods present degradation due to the fact that discrepancies between radar and rain gauge measurements are larger for such short aggregation periods (Sideris *et al.* 2014). The authors found that, in the context of real-time no-human-intervention applications, hourly input accumulations give a satisfactory balance between very high temporal resolution (non-robust), aggregations and very robust but low temporal resolution. Thus, as used in other geostatistical studies of QPE (Harberlandt 2007; Velasco-Forero *et al.* 2009; Verworn & Haberlandt 2011), 5 min rainfall values were aggregated to hourly values. Accumulated hourly radar images were computed assuming that precipitation fields move at a constant velocity between images and vary linearly in intensity with time between each interval (Bellon *et al.* 1991).

A map of false echoes was available, obtained on different clear days. To correct these false echoes, this map was automatically subtracted from each reflectivity image. It was later proven that for clear days without precipitation, the reflectivity image is almost white, with tiny echoes remaining which are usually present despite correction (Meischner 2004). Quantifying attenuation was difficult since this is not a polarimetric radar and there is no receiving antenna in the basin, but a comparison of different radar images for intense rain events confirmed that attenuation in the area was not significant. Furthermore, the radar was so close to the basin that attenuation would not be high.

According to the power law established by Marshall & Palmer (1948), the relation between dBZ (10 $\log_{10}$Z) and $\log_{10}$R must be linear. This renders it possible to obtain linear correlation maps (centered on a rain gauge) between $\log_{10}$R and dBZ at nearby pixels. In the absence of anomalous propagation, the most correlated point will be the center of the map, making it possible to compare rainfall data with reflectivity at rain gauge coordinates. When there are strong temperature inversions, the radar beam suffers super refraction and it bends toward the ground. In these situations, the most correlated point would show a radial displacement with respect to the gauge coordinates, indicating a problem of anomalous propagation (Bean & Dutton 1966; Pamment & Conway 1998; Fabry 2015).

It is important to note that the same approach employed by Goudenhoofdt & Delobbe (2009) and Velasco-Forero *et al.* (2009) was followed, and rainfall data were used in their original form rather than transforming them into Gaussian space.

Differentiation between stratiform and convective events

Another important and challenging issue affecting radar QPEs is related to the precipitation origin: either convective or stratiform events. Systematic discrimination between convective and stratiform events can be performed with different techniques (Anagnostou & Kummerow 1997; Awaka *et al.* 1997; Hong *et al.* 1999; Llasat 2001; Verworn & Haberlandt 2011; Nanding *et al.* 2015). Monjo (2016), using a dimensionless index to separate events by origin, defined according to the relative temporal distribution of maximum intensities. The main advantages of this method are that it does not require thresholds, so it can be applied for each rain gauge.

In order to obtain specific Z-R relations, rainfall was classified as predominately convective or stratiform based on its temporal variability within each hour, which is connected to the type of rainfall (convective/stratiform). In particular, the method described by Monjo (2016) was applied, taking maximum intensities recorded for different temporal resolutions and summarizing the relative concentration for each rainfall event: the ratio of two maximum averaged intensities (I_1/I_2) is equal to the inverse ratio of both temporal intervals (t_2/t_1), but to the power of a

dimensionless index (n) that ranges between 0 and 1 (Moncho *et al.* 2009):

$$\frac{I_1}{I_2} \approx \left(\frac{t_2}{t_1}\right)^n \tag{1}$$

Definition of the n index is based on the fact that stratiform rainfall (advective or frontal) normally has a constant intensity during all events, whereas convective rainfall is characterized by variable intensities within the same event. Therefore, n values close to 0 are associated with constant intensities (stratiform event), while values close to 1 indicate variable intensities of convective events. In the present study, hourly n indexes were computed for each rain gauge and the median of the n distribution was used as the threshold for considering rainfall as predominantly stratiform. Comparison of convective available potential energy values and n indexes classification validated the stratiform–convective separation in the present work.

Z-R equation

Z-R relations were fitted for X-band radar using a linear adjustment. R software (R Development Core Team 2013) was employed for these calculations. Expressing reflectivity Z in logarithmic scale as $Z'(dBZ) = 10 \log_{10} Z$, and using the Marshall-Palmer relation, $Z = a\ R^b$, yields:

$$R = 10^{\frac{Z' - 10\log_{10}a}{10b}} \tag{2}$$

For the $R(Z)$ fits, it was necessary to set initial points, which were computed for various significant events from the following linear regression:

$$\log_{10} R = \frac{1}{10b} Z' - \frac{\log_{10}a}{b} \tag{3}$$

The origin of this function (Equation (3)), defined as $O = \log_{10}(a)/b$, was fitted separately to determine the minimum level of radar sensitivity. In particular, reflectivity and precipitation values were taken from the smallest rainfall events and thus a value of O was obtained for each type of precipitation (e.g. convective or stratiform).

The approach employed to produce a universal merging scheme that can be run in all meteorological conditions was to identify convective and stratiform events automatically and adjust their Z-R relations separately (Figure 1).

Variogram estimation

All geostatistical interpolation methods require the estimation of model parameters of the spatial structure

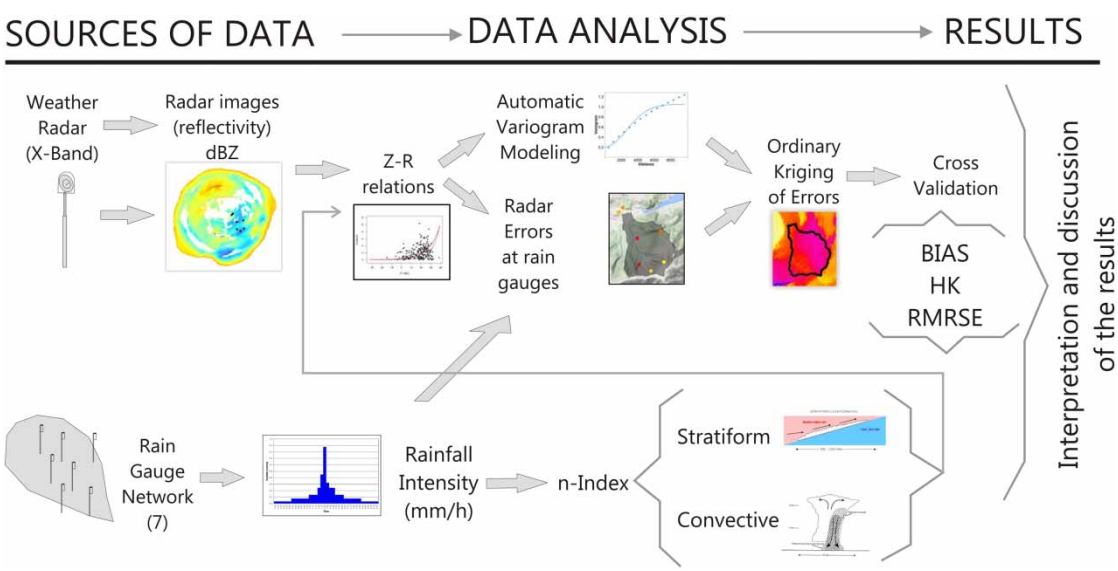

Figure 1 | Methodology scheme.

through variogram models. A variogram measures the spatial variability of a random process as a function of the distance between data pairs (Armstrong 1998):

$$\gamma(h) = \frac{1}{2N(h)} \sum_{x_i - x_j = h} \left(Z(x_i) - Z(x_j)\right)^2 \quad (4)$$

where $N(h)$ is the number of precipitation (Z) data pairs measured at locations x_i and x_j, which are located a distance vector h apart. Therefore, one particular problem for geostatistical interpolation of complete time series is effective and reliable estimation of the variograms for each time step. Variograms were inferred from radar rainfall data due to the higher spatial resolution compared with the recording stations.

A theoretical model must be fitted in order to deduce the variogram values for any possible distance required by interpolation algorithms (Goovaerts 2000). The variogram model was calculated for each time step, as each calculation time was treated independently from the previous ones. Hence, an automatic approach was applied with the geostatistical R package, *gstat* (Pebesma 2004), and the model type that best fit experimental variograms was established. The sill, nugget and range were determined by the fitting procedure. The sill is the upper boundary of the variogram function, equal to the variance of the underlying studied population. The nugget represents any discontinuity at zero separation and the range is the distance over which the covariance is valid (i.e. the extent of the spatial structure in the data).

Ordinary kriging of the errors

From among all the existing geostatistical algorithms (Ly *et al.* 2013), the algorithm chosen to combine radar and rain gauge data in real-time was OKRE (Erdin 2013). This method is analogous to the one reported first in Ehret (2003) and later developed as MERG in Sinclair & Pegram (2005). The main idea is to interpolate the radar-estimated errors at gauge locations (Figure 2). The first

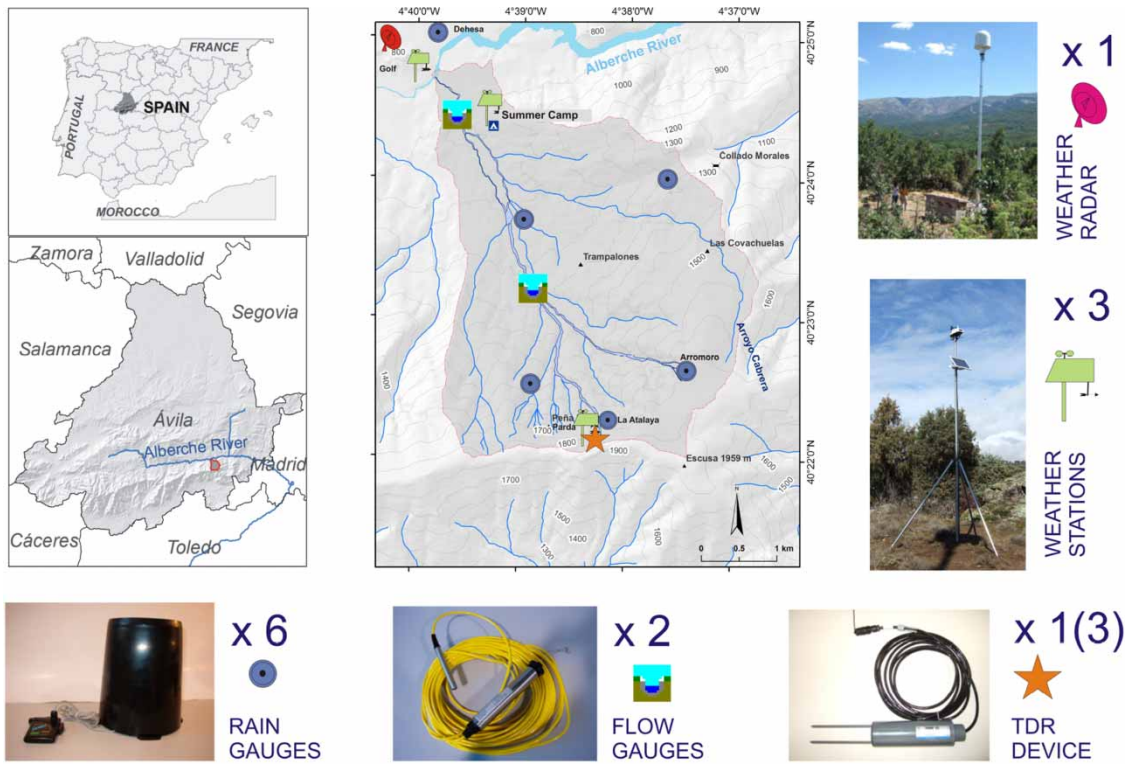

Figure 2 | Location map of the Venero Claro Basin.

step of the procedure was to estimate radar rainfall values from the *Z-R* equations obtained above (Equation (3)). Experimental variograms were computed from these radar rainfall field data (based only on radar data) and automatic variogram modeling was performed. Next, radar errors were determined by local radar-gauge comparison and interpolation with ordinary kriging using the variogram model of the radar rainfall field. This approach means, in terms commonly used in geostatistics, that rainfall is considered a regionalized variable (Armstrong 1998) and its trend is approximated as an external drift given by the radar. Then, residuals (Goovaerts 2000) correspond to what in this work is called radar errors. The spatial variability of the stationary part of the trend (radar) can be taken to model the spatial variability of the residuals.

This was then followed by subtracting the interpolated radar error from the radar rainfall values estimated from *Z-R* relations to obtain the actual precipitation estimate. Differences in the variogram structure between the radar and radar errors explain the miscalculations of the present method. Ordinary kriging was built using the geostatistical R package *gstat* (Pebesma 2004).

Validation

To validate the interpolation results, the 'leave-one-out' or cross-validation method was applied. A successive estimation of all gauge locations was performed by using all other stations and always omitting the sample value at the location in question. Three performance measures or scores were used to compare estimations and observations, as described below. The corresponding analysis is presented in the Results and discussion section.

Bias

Bias was computed to determine the presence of systematic errors that over- or underestimated precipitation. This error measure was defined as the ratio between the total estimated precipitation and the total observed precipitation, over all time steps and locations. This ratio is expressed in log scale (*d*B), as is frequent practice in radar meteorology (Erdin 2013):

$$\text{Bias } (d\text{B}) = 10 \log_{10}\left(\frac{\sum \text{estimated}}{\sum \text{observed}}\right) \tag{5}$$

Bias equal to 0 *d*B corresponds to a lack of over- or underestimation, while positive or negative bias values are indicative of over- and underestimation, respectively. This measure gives the factor of under- or overestimation by conversion of the logarithmic scale. For example, +2 *d*B corresponds to an overestimation by a factor of 1.58.

Hanssen-Kuipers discriminant

The Hanssen-Kuiper (HK) skill score (Peirce 1884), sometimes called the HK discriminant or the true skill statistic, is defined by:

$$HK = \frac{AD - BC}{(A + C)(B + D)} \tag{6}$$

where A, B, C and D are the number of records described in Table 1.

This was employed to distinguish between dry and wet areas. The term discriminant that is sometimes used refers to this score's characteristic of measuring discrimination between yes and no cases. The score has a range of −1 to +1, where 0 represents no skill or a random estimate and 1 represents a perfect estimate. *HK* is also the difference between the hit rate and false rain rate. Therefore, it makes it possible to examine whether forecasting an event, particularly a rare event, more often leads to a large increase in false rains or not.

Relative mean root transformed error

Erdin (2013) defined the relative mean root transformed error (*RMRTE*) to quantify the overall performance of the

Table 1 | Combinations between success and failure when predicting rain and no rain records in the rain gauges

	Rain observation	No rain observation
Rain estimation	*A*	*B*
No rain estimation	*C*	*D*

estimation:

$$RMRTE = \frac{\frac{1}{n}\sum_{i=1}^{n}\left(\sqrt{est_i} - \sqrt{obs_i}\right)^2}{\frac{1}{n}\sum_{i=1}^{n}\left(\sqrt{obs_i} - \overline{\sqrt{obs}}\right)^2} \quad (7)$$

This is similar to a root-mean-squared error, but is adapted to the skewed nature of precipitation. This behavior is reflected in the fact that intense events are less predictable than light precipitations or dry records. In addition, it is normalized by the mean root-squared deviation in order to mitigate dependency on the observed precipitation deviation. $RMRTE = 0$ indicates a perfect estimation, whereas $RMRTE = 1$ is equivalent to approximate precipitation with the mean rainfall value.

Study area and data

The study area, the Venero Claro Basin (Ávila, Spain), has suffered severe flash floods in the past, and these thus need to be predicted in order to improve awareness measures and mitigate future damage. Although the catchment (Figure 2) may appear to have a high density of instruments, six rain gauges are still not enough to directly derive spatial variability in rainfall. Venero Claro is the drainage basin of the La Cabrera Stream, which measures 5.5 km long, and it covers an area of 15.5 km^2 with a maximum altitude difference of 1,224 m between the highest point (1,959 m a.s.l.) and to the point where the stream flows into the Alberche River (735 m a.s.l.). The average slope of the stream is 21.6%. Geologically, the area is located in the western part of the Spanish Central System. The bedrock consists of biotite granites and granodiorites from intrusions during the Variscan orogeny. Superficial Quaternary formations are made up of gravels, sands and silts. These cover the slopes, the valley bottom and endorheic depressions. Its morphology and composition is common to other small catchments in the Spanish Central System.

The climate of the study area is Continental Mediterranean, which is typical of inland Spanish mountain ranges. The climate of these mountains is determined by the frequent arrival of Atlantic depressions, mainly from the SW, during fall, winter and spring, and by the predominant Azores anticyclone which causes very dry summers (accounting for only 10% of the annual precipitation). The mean annual precipitation is 554 mm in the lower areas and up to 2,000 mm at the highest point (Palacios *et al.* 2011). Six recording stations provided continuous rainfall data between 2006 and 2014 over 5 minute time intervals. Rain gauge values are considered as estimates of true precipitation rate at the station location. In this study area there is a sparse rain gauge density when compared to the spatial variability of precipitation (Ruiz-Villanueva *et al.* 2011, 2013). During the rainfall data period, 6,006 hours had at least one rain gauge measuring. Only five rain gauges were operating during rainfall events with radar data (317 hours with rain measured by at least one rain gauge and with reflectivity images).

An X-band weather radar was installed in 2012, located 2,330 m west of the mouth of the La Cabrera Stream (Figure 2). This is an appropriate location as it is close enough to avoid strong attenuations and the radar is able to cover the entire vertical profile of the basin, with a fixed elevation angle of 12°. The technical specifications of

Table 2 | Technical data of the X-band radar located in the Venero Claro Basin

Model	Rainscanner Radar System RS90. Selex-SI Gematronik	Nominal horizontal range	50 km
Instantaneous power pulse	25 kW	Pulse duration	1,200 ns
Wavelength	3.19 cm	Beam with	2.5°
Frequency	9.4 ± 0.3 GHz	Pulse length	180 m
Pulse repetition frequency	833 Hz	Dip (from the horizon)	12 °
Single polarization	horizontal	Radome losses	0.4 dB
Transmit path loss	0.5 dB	Receive path loss	0.5 dB

the radar are given in Table 2. Recording spatial resolution was defined as 80×80 m or 120×120 m, while time resolution was 5 min. A region of 50×50 km centered on the radar was defined as the study area.

RESULTS AND DISCUSSION

Stratiform or convective origin of precipitation

The index n, used to discriminate between convective or stratiform events, was computed for all the measured hours and rain gauges. The median of n was quite similar for all the locations, ranging from 0.38 to 0.46, and no relation between n and altitude was found (upper plot of Figure 3). When a Kolmogorov–Smirnov test was performed, the probability distribution function of n had a Gumbel shape with a median value around 0.4. This median value coincided with the theoretical threshold used to distinguish between convective and stratiform origin. With this criterion, 131 of the 317 hourly data were classified as convective and 186 as stratiform. In middle latitudes, convective events occur during periods in which surface heating is greater, giving more stormy phenomena and more irregular rain. This fact is illustrated in Figure 3 (lower plot), in which the months of greatest warming were characterized by higher n index values.

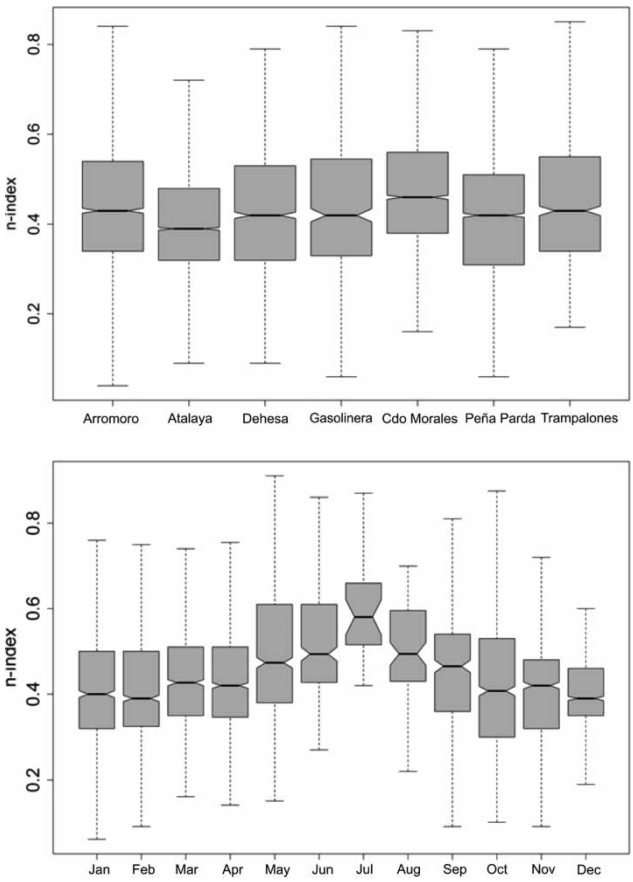

Figure 3 | Box plots of hourly n indexes obtained at each rain gauge (upper plot) and hourly n indexes at all the rain gauges differentiating by month (lower plot). Gasolinera rain gauge is located 300 m east of Dehesa rain gauge, 100 m out of the area shown in Figure 2.

The Z-R relation obtained with the linear fit gave values of $a = 24.1$ and $b = 2.6$ for stratiform events, and $a = 47.5$ and $b = 3.2$ for convective ones (Figure 4). For X-band radar, Van de Beek *et al.* (2010) obtained different Z-R relations in an area close to Delft (The Netherlands): $a = 120$ and $b = 1.57$ for stratiform events, and $a = 40$ and $b = 2.07$ for convective origin of rain. They classified on the basis of visual inspection of all events, rather than by means of an objective tool such as the one used in the present study. Another difference between the current study and that of Van de Beek *et al.* (2010) is that the method chosen to adjust Z-R relations was a linear fit, whereas Van de Beek *et al.* found that non-linear approximation gave the best results. These dissimilarities in the method and the differences in the orography of the two studies explain the variations in a and b values. Van de Beek *et al.* (2010) studied flat terrain, whereas the Venero Claro Basin is a steep mountainous area. The elevation angle of 12° also affected the measurement of precipitation on the ground, mostly in gauges located at medium distances and at a similar altitude to the radar.

Precipitation estimation from X-band radar with OKRE

Regarding radar data analysis, the existence of anomalous propagation was investigated by looking for displacement patterns in the radar data. Generally, the best correlated pixel was the one corresponding to the gauge. Hence, no anomalous propagation correction was required. Due to the low number of rain gauges, it was not possible to apply the MERG or KED method as no variogram model could be inferred for rainfall. In contrast to Erdin (2013),

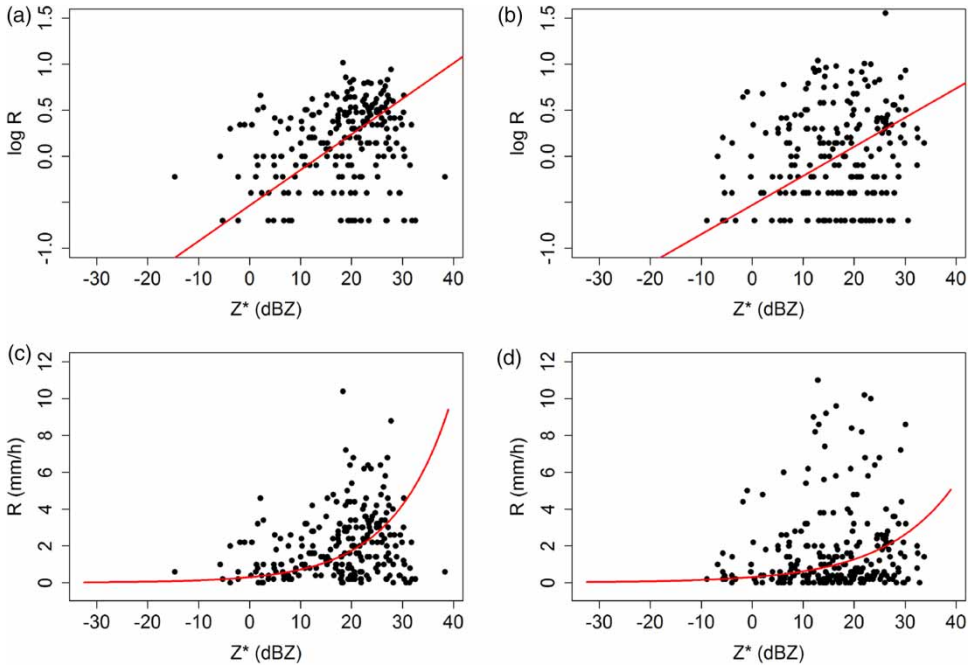

Figure 4 | In red, linear fits for log(*R*)-*Z'*, differentiating between stratiform, (a) and (c), and convective events, (b) and (d). Please refer to the online version of this paper to see this figure in colour: http://dx.doi.org/10.2166/hydro.2016.225.

rainfall data were not transformed in the present application of OKRE.

The lack of knowledge about spatial rainfall variability is one of the major sources of uncertainty in the stream flow model-derived information (Willem & Berlamont 2002). Hence, even if there are not as many rain gauges as in the applications of OKRE performed by Erdin (2013) with 75 rain gauges or by Nanding *et al.* (2015) with up to 161 rain gauges, the study of the flood predictions in the area needs to improve as much as possible the spatial heterogeneities of QPE. In the present work it is possible to avoid the reduction of the significance of the results due to the small number of gauges by taking the radar correction variability directly from the radar data. Assigning radar spatial variability to rainfall spatial variability will end up in some uncertainties on the results. However, the reduction on the uncertainty linked to the experimental variogram justifies this assumption. It may be here recalled that the experimental variogram is statistically robust when it is computed from a minimum of 30 data pairs (Journel & Huijbregts 1978). Similarly, Germann & Joss (2001) conducted precipitation variogram estimation using radar data and reported that high resolution radar images provided good information about the spatial continuity of precipitation. The same approach was taken by Berndt *et al.* (2014). The novelty of the methodology proposed here is the application of OKRE using the radar variogram model to krige the radar errors.

Theoretically, variogram estimation must be carried out separately for each time step. If this is done manually, the procedure is very time-consuming and subjective. A solution proposed by Schuurmans *et al.* (2007) is to use pooled variogram models based on all the studied events. They recommended this practice when there is a lack of data or when an automatic prediction procedure is implemented without variogram estimation. Berndt *et al.* (2014) and Rabiei & Haberlandt (2015) used seasonal variogram models, averaging variograms for all time steps within each of the two split seasons. Other authors such as Velasco-Forero *et al.* (2009) have used non-parametric automatic evaluation of the variogram model for each time step. In the present study, fitting a parametric variogram for each hour of estimation was considered of great importance to capture temporal variation in rainfall. As with Schuurmans

et al. (2007) and Erdin (2013), automatic experimental calculation and modeling of the variogram was successfully implemented. Previous research by Ehret (2003); Verworn & Haberlandt (2011) and Erdin (2013) showed that the choice of variogram model had little impact on rainfall estimation performance. In this work, after different trials, the variogram model selected as the best option was the Gaussian model.

Figure 5 shows the rainfall field interpolated by using OKRE, for one case study (18:00 UTC, 28 September 2012). The average n index for this time step in all the rain gauges was 0.34, and the rainfall was classified as stratiform. A qualitative analysis of the image showed that OKRE was effective at maintaining the fine details of the radar data, highlighting that the addition of radar information is very important when not all the gauges are registering rainfall.

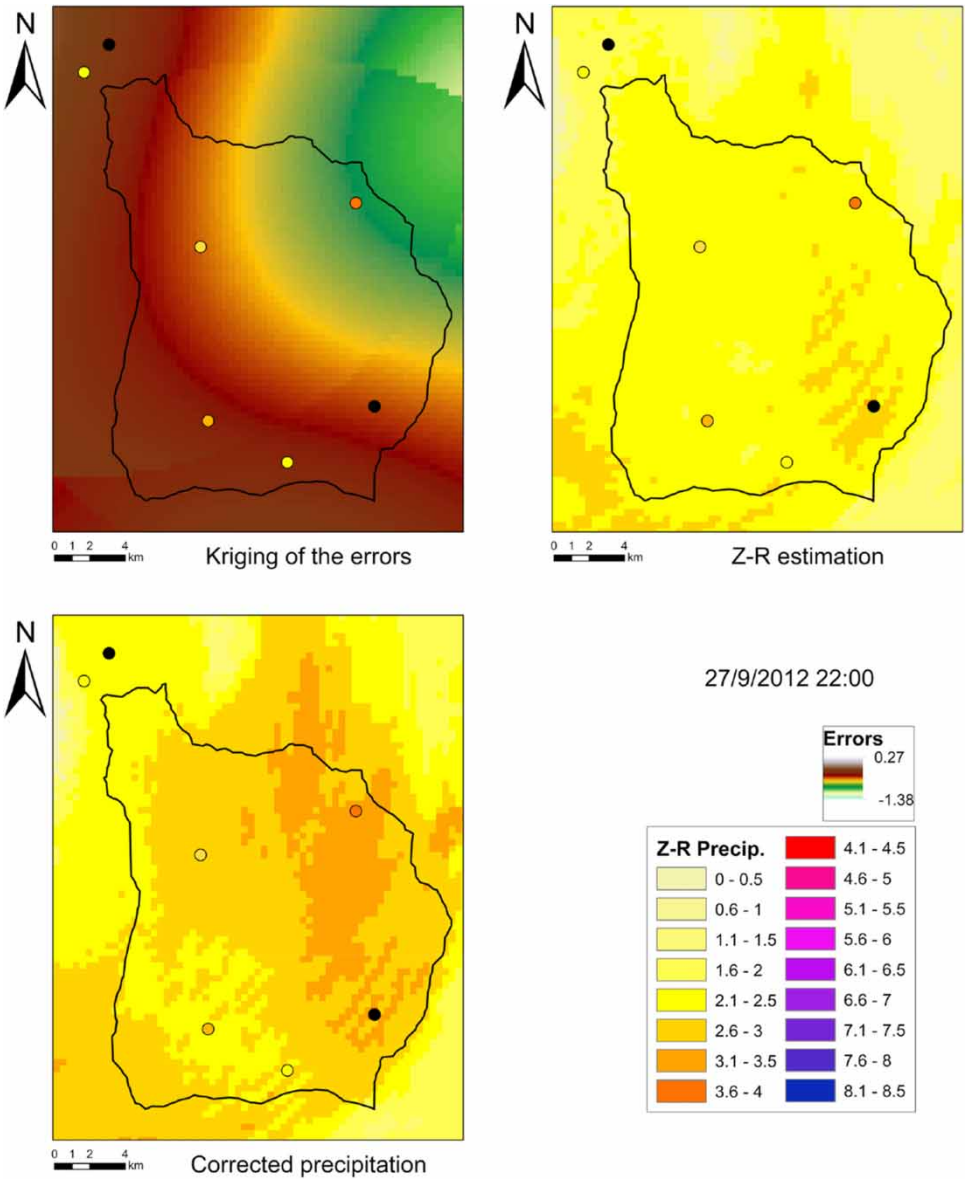

Figure 5 | Interpolated rainfall maps at UTM coordinates obtained for 18:00 UTC, 28 September 2012, initial estimation was obtained from the linear *Z-R* fit, and radar errors were computed with the OKRE method. This field was subtracted from the initial one and the corrected values gave the new estimation. Points correspond to the rain gauge locations, black points indicate the value was not available for this time.

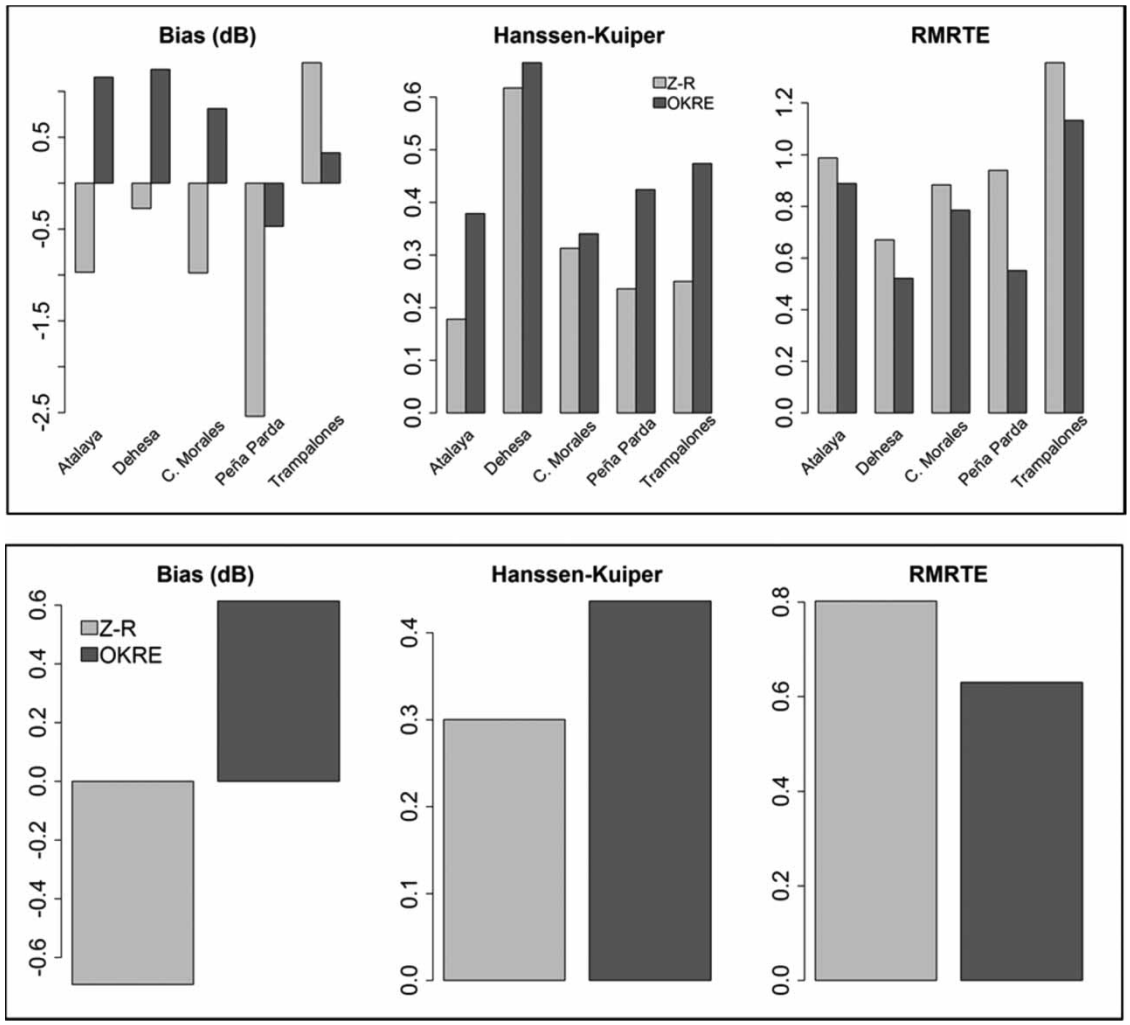

Figure 6 | Bias (*dB*), *HK* discriminant and *RMRTE* evaluated for all the available data (lower plot) and differentiating for the five rain gauges (upper plot).

Figure 6 shows the error scores computed for each of the rain gauges separately (upper plot) and in conjunction (lower plot). Estimated values using *Z-R* relations underestimated rainfall, whereas OKRE overestimated it by 15%. This bias is attributed to the OKRE design implemented here. Approximating the variogram of the errors by the variogram of the radar introduces some errors into the estimation. On the other hand, when only one rain gauge is measuring, the radar correction obtained at this point is taken for the entire image, and it is not possible to perform interpolation. This is where the OKRE method differs from the MERG method described by Sinclair & Pegram (2005): in MERG, if there are radar values at more than one rain gauge, these values are interpolated at radar locations (even when only one rain gauge is measuring) and then compared to the original radar field.

Bias values differ considerably between rain gauge locations. The only rain gauge for which OKRE gave a slight underestimation was the one located at the top of the basin (Peña Parda in Figure 6). This can be explained by the fact that when it was raining at this point, it also rained in the rest of the basin, but probably with less intensity. In these cases, interpolation was always performed taking into account smaller rainfall values. The elevation of the radar, 12°, also affected the reflectivity measurements, being less accurate at higher elevations.

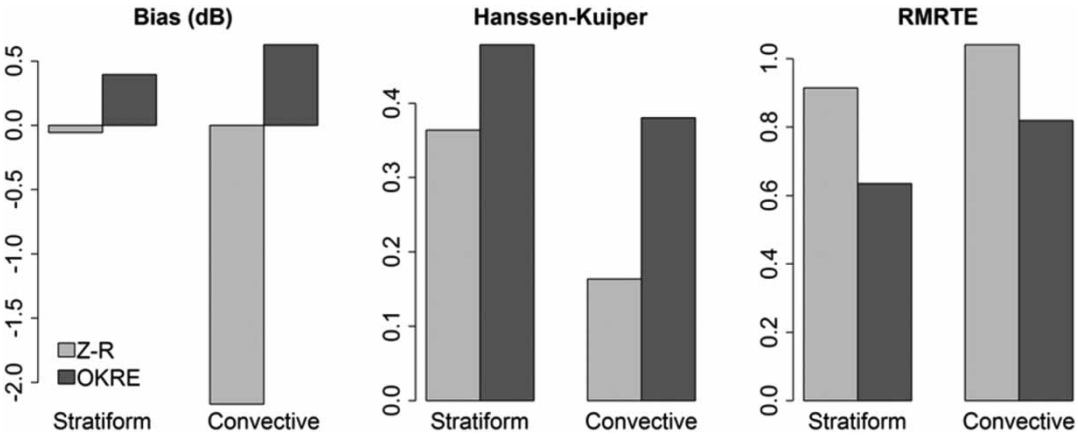

Figure 7 | Bias (*dB*), *HK* discriminant and *RMRTE* evaluated for all the available data differentiating between convective and stratiform events.

Globally, *HK* values were much improved (closer to 1) with OKRE (Figure 7). The superior performance of OKRE with respect to wet-dry distinction was also observed by Erdin (2013) in comparison with KED. The two gauges closest to the radar and at a lower altitude (Dehesa and Trampalones) yielded better *HK* values. Again, this is attributed to the elevation of the radar, which is already the optimal angle: smaller angles could make the beam intersect with the ground, and larger ones might leave out orographic induced rainfall on the ridge.

With regard to the *RMRTE*, an improvement was achieved with the geostatistical method in comparison with the *Z-R* relation. The best estimations were obtained at the Dehesa location (closest to the radar). This good performance of the method with X-band radar data was also observed with C-band radar information by Ehret *et al.* (2008) and Nanding *et al.* (2015) when using the similar MERG method. Ehret *et al.* (2008) reported that MERG gave better results than when using only radar data with a static or updated *Z-R* relation, when using radar but determining the *Z-R* relation with a disdrometer, or when using KED.

Variogram analysis

Valuable information was extracted from the stratiform and convective ensembles of variogram models. The Gaussian model parameters were analyzed to determine characteristics of spatial continuity that differentiated stratiform and convective events, and quartiles of parameters in both ensembles were computed (Table 3). Sill median values were not very different for the two kinds of event (0.13 for convective and 0.40 for stratiform). The higher sill values for stratiform events (Q2 0.4 and Q3 3.73) indicated higher hourly precipitations than convective ones (Q2 0.13 and Q3 0.39). Median range values indicated that stratiform events in the area had a spatial correlation up to ~5 km, whereas this was up to ~4 km for convective events. This higher correlation length is explained by the larger dimensions of the stratiform rain processes, corroborating the consistency of the methodology. Similar characteristics can be seen in the experimental variograms shown in Jewell & Gaussiat (2015) for convective and stratiform events.

Table 3 | Quartiles of variogram model parameters in classified convective and stratiform events. A Gaussian model was used for all the events

	Nugget convective	Nugget stratiform	Sill convective	Sill stratiform	Range convective	Range stratiform
Min.	0.00	0.00	0.00	0.00	572.30	1,037.26
Q1	0.01	0.01	0.02	0.00	2,307.69	2,847.96
Q2	0.02	0.03	0.13	0.40	4,079.50	5,077.84
Q3	0.03	0.11	0.39	3.73	5,555.40	13,951.56
Max.	0.12	0.52	18.32	125.78	257,430.66	328,056.59

Figure 7 shows the three error scores obtained for all the points and times, but distinguishing between stratiform and convective origin. For the estimation using *Z-R* relations and no geostatistical merging, the bias error measurement indicated that it was almost unbiased for stratiform rainfalls, but highly underestimated for convective ones. This can also be seen in Figure 4, where points of higher intensity are far from the adjustment. This underestimation of spatially distributed precipitation estimates is confirmed by other authors (Van de Beek *et al.* 2010; Thorndahl *et al.* 2014; Nanding *et al.* 2015; Rabiei & Haberlandt 2015), and is particularly dangerous when predicting flash floods during convective events. When using *Z-R* adjustments, the probability of successfully distinguishing wet and dry periods (*HK*) is much higher in stratiform events compared with convective ones. For both rain origins, *HK* was much improved in the OKRE results. Error values computed with the *RMRTE* for estimations applying the *Z-R* estimations were very high, reaching the value of 1, and hence estimated values were comparable with the average precipitation of all rain gauges. These *RMRTE*'s were also much improved by means of OKRE.

In general, the geostatistical method described here yielded better predictions of stratiform events than of convective ones. In comparison with stratiform rainfall, convective events presented higher overestimations, worse discrimination between dry and wet periods and a larger *RMRTE*. This has been also found by Velasco-Forero *et al.* (2009), Erdin (2013), Legorgeu (2013), Jewell & Gaussiat (2015), among many others. It remains to be determined how significant this improvement is in terms of rainfall product resolution and accuracy in flood simulations for this basin. As was also observed by Van de Beek *et al.* (2010); Verworn & Haberlandt (2011) and Jewell & Gaussiat (2015), the results obtained highlight the importance of meteorological conditions on the quality of the merged product.

CONCLUSIONS

The main innovation of the present work is the application of a merging radar-rain method to a small catchment (15 km^2) with very small concentration times, where only a dense rain gauge network (e.g. 10 times higher than the World Meteorological Organization recommendations for small mountainous islands with irregular precipitation) combined with one X-band radar with a high spatial resolution, allows an adequate characterization of precipitation. Cross-validation results throughout the basin and the data proved a good performance of the interpolation approach. In comparison with the classical *Z-R* relationships, obtained here from a linear fit, the method described here showed a greater capacity for distinguishing between wet and dry areas and only presented minor errors in the estimate with respect to the observed values.

Another novel aspect of this work was the use of the *n* index to improve the *Z-R* adjustment for convective and stratiform precipitation. The main advantages of this method are that it does not require thresholds, so it can be applied for each rain gauge. Moreover, this index allows automatic separate variogram modeling of stratiform and convective events, which opens up new possibilities for further investigating the consequences of this separation.

This classification of rainfall origin, which is also the contribution of the proposed method in comparison with other similar studies using OKRE, is implemented in the real-time QPE estimation process. The present study shows that QPE in convective events involved larger errors than for stratiform events. This finding may, in part, be explained by the greater spatial irregularity of convective precipitation, corroborated by the modeled variogram ranges. Moreover, spatial correlation for convective events can be characterized up to ~4 km, while for stratiform events up to ~5 km, both values taken from the median ranges of all fitted models.

Further research could involve using more sophisticated algorithms such as KED and parametric variogram modeling. Another future application of these variogram models would be the simulation or disaggregation of convective and stratiform events. This study has provided the basis for subsequent hydrological calibration and validation based on rainfall runoff modeling, while also offering a methodology that can be applied in basins with similar characteristics.

ACKNOWLEDGEMENTS

X-band radar installation was funded by the FEDER project UNCM08-1E-086. This study also forms part of the

MARCoNI project (funded by the Spanish Ministry of Economy and Competitiveness, ref: CGL2013-42728-R), the MIDHATO Venero project (funded by the Spanish Geological Survey, ref: IGME 2313/2010) and projects CGL2013-48367-P and CGL2016-80609-R (funded by the Spanish Ministry of Economy and Competitiveness). We would also like to thank technicians and rangers from the Regional Government of Castile and León, Navaluenga City Council and the Fundación Caja de Ávila, for their essential support during the study.

REFERENCES

Anagnostou, E. N. & Kummerow, C. 1997 Stratiform and convective classification of rainfall using SSM/I 85-GHz brightness temperature observations. *Journal of Atmospheric and Oceanic Technology* 14, 570–575.

Anagnostou, M. N., Kalogiros, J., Anagnostou, E. N., Tarolli, M., Papadopoulos, A. & Borga, M. 2010 Performance evaluation of high-resolution rainfall estimation by X-band dual-polarization radar for flash flood applications in mountainous basins. *Journal of Hydrology* **394**, 4–16.

Armstrong, M. 1998 *Basic Linear Geostatistics*. Springer-Verlag, Heidelberg.

Awaka, J., Iguchi, T., Kumagai, H. & Okamoto, K. 1997 Rain type classification algorithm for TRMM precipitation radar. In: *Geoscience and Remote Sensing, IEEE International*, 4, pp. 1633–1635.

Bean, B. R. & Dutton, E. J. 1966 *Radio Meteorology,* National Bureau of Standards Monograph No. 92. US Government Printing Office, Washington.

Bellon, A., Fabry, F. & Austin, G. L. 1991 Errors due to space/time sampling strategies in high resolution radar data used in hydrology. In: *25th Radar Meteorology Conference, American Meteorology Society*, Paris, pp. 2040–2048.

Berndt, C., Rabiei, E. & Haberlandt, U. 2014 Geostatistical merging of rain gauge and radar data for high temporal resolutions and various station density scenarios. *Journal of Hydrology* **508**, 88–101.

Borga, M. 2002 Accuracy of radar rainfall estimates for streamflow simulation. *Journal of Hydrology* **267**, 26–39.

Carrera-Hernandez, J. J. & Gaskin, S. J. 2007 Spatio temporal analysis of daily precipitation and temperature in the Basin of Mexico. *Journal of Hydrology* **336**, 231–249.

Chappell, A., Renzullo, L. J., Raupach, T. H. & Haylock, M. 2013 Evaluating geostatistical methods of blending satellite and gauge data to estimate near real-time daily rainfall for Australia. *Journal of Hydrology* **493**, 105–114.

Cole, S. J. & Moore, R. J. 2008 Hydrological modelling using raingauge- and radar-based estimators of areal rainfall. *Journal of Hydrology* **358**, 159–181.

Creutin, J. D. & Obled, C. 1982 Objective analyses and mapping techniques for rainfall fields: an objective comparison. *Water Resources Research* **18**, 413–431.

Creutin, J. D., Delrieu, G. & Lebel, T. 1988 Rain measurement by raingauge-radar combination: a geostatistical approach. *Journal of Atmospheric and Oceanic Technology* **5**, 102–115.

Delrieu, G., Caoudal, S. & Creutin, J. D. 1997 Feasibility of using mountain return for the correction of ground-based X-band weather radar data. *Journal of Atmospheric and Oceanic Technology* **14**, 368–385.

Ehret, U. 2003 *Rainfall and Flood Nowcasting in Small Catchments Using Weather Radar,* 1st edn. Mitteilungen. Eigenverlag des Instituts für Wasserbau der Universität Stuttgart, Stuttgart.

Ehret, U., Götzinger, J., Bardossy, A. & Pegram, G. 2008 Radar-based flood forecasting in small catchments, exemplified by the Goldersbach catchment, Germany. *International Journal of River Basin Management* **6**, 323–329.

Erdin, R. 2013 *Geostatistical Methods for Hourly Radar-Gauge Combination: An Explorative, Systematic Application at MeteoSwiss*, Scientific Report. MeteoSwiss 92.

Fabry, F. 2015 *Radar Meteorology. Principles and Practice.* Cambridge University Press, New York.

Germann, U. & Joss, J. 2001 Variograms of radar reflectivity to describe the spatial continuity of Alpine precipitation. *Journal of Applied Meteorology* **40**, 1042–1059.

Germann, U., Berenguer, M., Sempere-Torres, D. & Zappa, M. 2009 REAL—ensemble radar precipitation estimation for hydrology in a mountainous region. *Quarterly Journal of the Royal Meteorological Society* **135**, 445–456.

Gires, A., Schertzer, D., Tchiguirinskaia, I., Lovejoy, S., Onof, C., Maksimovic, C. & Simoes, N. 2012 Impact of small scale rainfall uncertainty on urban discharge forecasts. In: *Weather Radar and Hydrology Symposium*, IAHS Publ. 351, pp. 400–406.

Goovaerts, P. 2000 Geostatistical approaches for incorporating elevation into the spatial interpolation of rainfall. *Journal of Hydrology* **228**, 113–129.

Goudenhoofdt, E. & Delobbe, L. 2009 Evaluation of radar-gauge merging methods for quantitative precipitation estimates. *Hydrology and Earth System Sciences* **13**, 195–203.

Gourley, J. J., Hong, Y., Flaming, Z. L., Wang, J., Vergara, H. & Anagnostou, E. N. 2011 Hydrologic evaluation of rainfall estimates from radar, satellite, gauge, and combinations on F. Cobb Basin, Oklahoma. *Journal of Hydrometeorology* **12**, 973–988.

Grimes, D. I. F., Pardo-Iguzquiza, E. & Bonifacio, R. 1999 Optimal areal rainfall estimation using raingauges and satellite data. *Journal of Hydrology* **222**, 93–108.

Harberlandt, U. 2007 Geostatistical interpolation of hourly precipitation from rain gauges and radar for a large-scale extreme rainfall event. *Journal of Hydrology* **332**, 144–157.

Heistermann, M. & Kneis, D. 2011 Benchmarking quantitative precipitation estimation by conceptual rainfall-runoff modeling. *Water Resources Research* **47**. doi:10.1029/2011WR010617.

Hong, Y. & Gourley, J. J. 2015 *Radar Hydrology: Principles, Models, and Applications*. CRC Press, Boca Raton.

Hong, Y., Kummerow, C. & Olson, W. S. 1999 Separation of convective and stratiform precipitation using microwave brightness temperature. *Journal of Applied Meteorology* **38**, 1195–1213.

Jewell, S. A. & Gaussiat, N. 2015 An assessment of Kriging based rain-gauge–radar merging techniques. *Quarterly Journal of the Royal Meteorological Society*. doi: 10.1002/qj.2522.

Journel, A. G. & Huijbregts, C. J. 1978 *Mining Geostatistics*. Academic Press, London.

Krajewski, W. F. 1987 Cokriging radar-rainfall and rain gage data. *Journal of Geophysical Research: Atmospheres* **92** (D8), 9571–9580.

Krajewski, W. F., Kruger, A., Smith, J. A., Lawrence, R., Gunyon, C., Goska, R., Seo, B., Domaszczynski, P., Baeck, M. L., Ramamurthy, M. K., Weber, J., Bradley, A. A., DelCreco, S. A. & Steiner, M. 2011 Towards better utilization of NEXRAD data in hydrology: an overview of hydro-NEXRAD. *Journal of Hydroinformatics* **13**, 255–266.

Kyriakidis, P. C., Kim, J. & Miller, N. L. 2001 Geostatistical mapping of precipitation from rain gauge data using atmospheric and terrain characteristics. *Journal of Applied Meteorology* **40**, 1855–1877.

Lee, H., Zhang, Y., Seo, D., Kuligowski, R. J., Kitzmiller, D. & Corby, R. 2014 Utility of SCaMPR satellite versus ground-based quantitative precipitation estimates in operational flood forecasting: the effects of TRMM data ingest. *Journal of Hydrometeorology*. doi: 10.1175/JHM-D-12-0151.1.

Legorgeu, C. 2013 *Amélioration des estimations quantitatives des précipitations à hautes résolutions: comparaison de deux techniques combinant les observations et application à la vérification spatiale des modèles météorologiques (Improved Quantitative Estimates of Precipitation at High Resolutions: Comparison of two Techniques Combining Observations and Application to Spatial Checking Weather Patterns)*. PhD Thesis, Université Blaise Pascal – Clermont-Ferrand II, France (in French).

Llasat, M. C. 2001 An objective classification of rainfall events on the basis of their convective features: application to rainfall intensity in the northeast of Spain. *International Journal of Climatology* **21**, 1385–1400.

Lloyd, C. D. 2005 Assessing the effect of integrating elevation data into the estimation of monthly precipitation in Great Britain. *Journal of Hydrology* **308**, 128–150.

Ly, S., Charles, C. & Degré, A. 2013 Different methods for spatial interpolation of rainfall data for operational hydrology and hydrological modeling at watershed scale: a review. *Biotechnology Agronomy, Society and Environment* **17**, 392–406.

Marshall, J. S. & Palmer, W. 1948 The distribution of raindrops with size. *Journal of Meteorology* **5**, 165–166.

Meischner, P. 2004 *Weather Radar: Principles and Advanced Applications*. Springer-Verlag, Berlin.

Moncho, R., Belda, F. & Caselles, V. 2009 Climatic study of the exponent '*n*' in IDF curves: application for the Iberian Peninsula. *Tethys* **6**, 3–14.

Monjo, R. 2016 Measure of rainfall time structure using the dimensionless n-index. *Climate Research* **67**, 71–86.

Nanding, N., Rico-Ramirez, M. A. & Han, D. 2015 Comparison of different radar-raingauge rainfall merging techniques. *Journal of Hydroinformatics* **17**, 422–444.

Palacios, D., Marcos, J. & Vázquez-Selem, L. 2011 Last glacial maximum and deglaciation of Sierra de Gredos, Central Iberian Peninsula. *Quaternary International* **233**, 16–26.

Pamment, J. A. & Conway, B. J. 1998 Objective identification of echoes due to anomalous propagation in weather radar data. *Journal of Atmospheric and Oceanic Technology* **15**, 98–113.

Pebesma, E. J. 2004 Multivariable geostatistics in S: the gstat package. *Computers & Geosciences* **30**, 683–691.

Peirce, C. S. 1884 The numerical measure of the success of predictions. *Science* **4**, 453–454.

Rabiei, E. & Haberlandt, U. 2015 Applying bias correction for merging rain gauge and radar data. *Journal of Hydrology* **522**, 544–557.

R Development Core Team 2013 *R: A Language and Environment for Statistical Computing. R Foundation for Statistical Computing*, Vienna, Austria. http://www.R-project.org/ (accessed 1 July 2015).

Rico-Ramirez, M. A., Cluckie, I. D., Shepherd, G. & Pallot, A. 2007 A high-resolution radar experiment on the island of Jersey. *Meteorological Applications* **14**, 117–129.

Rogers, R. R. & Yau, M. K. 1989 *A Short Course in Cloud Physics*. International Series in Natural Philosophy, 3rd edn. Elsevier, New York.

Ruiz-Villanueva, V., Bodoque, J. M., Díez-Herrero, A. & Calvo, C. M. 2011 Triggering threshold precipitation and soil hydrological characteristics of shallow landslides in granitic landscapes. *Geomorphology* **133**, 178–189.

Ruiz-Villanueva, V., Bodoque, J. M., Díez-Herrero, A., Eguibar, M. A. & Pardo-Igúzquiza, E. 2013 Reconstruction of a flash flood with large wood transport and its influence on hazard patterns in an ungauged mountain basin. *Hydrological Processes* **27**, 3424–3437.

Schuurmans, J. M., Bierkens, M. F. P., Pebesma, E. J. & Uijlenhoet, R. 2007 Automatic prediction of high-resolution daily rainfall fields for multiple extents: the potential of operational radar. *Journal of Hydrometeorology* **8**, 1204–1224.

Seo, D. J. 1998 Real-time estimation of rainfall fields using radar rainfall and rain gage data. *Journal of Hydrology* **208**, 37–52.

Seo, D. J., Krajewski, W. F. & Bowles, D. S. 1990 Stochastic interpolation of rainfall data from rain gages and radar using cokriging: 1. Design of experiments. *Water Resources Research* **26**, 469–477.

Shrestha, N. K., Goormans, R. & Willems, P. 2013 Evaluating the accuracy of C- and X-band weather radars and their application for stream flow simulation. *Journal of Hydroinformatics* **15**, 1121–1136.

Sideris, I. V., Gabella, M., Erdin, R. & Germann, U. 2014 Real-time radar–rain-gauge merging using spatio-temporal cokriging with external drift in the alpine terrain of Switzerland. *Quarterly Journal of Royal Meteorological Society* **140** (680), 1097–1111.

Sinclair, S. & Pegram, G. 2005 Combining radar and rain gauge rainfall estimates using conditional merging. *Atmospheric Science Letters* **6**, 19–22.

Thorndahl, S., Nielsen, J. E. & Rasmussen, M. R. 2014 Bias adjustment and advection interpolation of long-term high resolution radar rainfall series. *Journal of Hydrology* **508**, 214–226.

Van de Beek, C. Z., Leijnse, H., Stricker, J. N. M., Uijlenhoet, R. & Russchenberg, H. W. J. 2010 Performance of high-resolution X-band radar for rainfall measurement in The Netherlands. *Hydrology and Earth System Sciences* **14**, 205–221.

Velasco-Forero, C. A., Sempere-Torres, D., Cassiraga, E. F. & Gómez-Hernández, J. J. 2009 A non-parametric automatic blending methodology to estimate rainfall fields from rain gauge and radar data. *Advances in Water Resources* **32**, 986–1002.

Verworn, A. & Haberlandt, U. 2011 Spatial interpolation of hourly rainfall–effect of additional information, variogram inference and storm properties. *Hydrology and Earth System Sciences* **15**, 569–584.

Villarini, G., Mandapaka, P., Krajewski, W. & Moore, R. 2008 Rainfall and sampling uncertainties: a rain gauge perspective. *Journal of Geophysical Research: Atmospheres* **113** (D11), doi: 10.1029/2007JD009214.

Webster, R. & Oliver, M. A. 1993 How large a sample is needed to estimate the regional variogram adequately? In: *Geostatistics Troia '92* (A. Soares, ed.). Vol 1, Kluwer Academic Publishers, Dordrecht, pp. 155–166.

Willem, P. & Berlamont, J. 2002 Accounting for the spatial rainfall variability in urban modelling applications. *Water Science & Technology* **45** (2), 105–112.

Zhang, Y., Reed, S. & Kitzmiller, D. 2011 Effects of retrospective gauge-based readjustment of multisensor precipitation estimates on hydrologic simulations. *Journal of Hydrometeorology* **12**, 429–443.

Zoccatelli, D., Borga, M., Zanon, F., Antonescu, B. & Stancalie, G. 2010 Which rainfall spatial information for flash flood response modelling? A numerical investigation based on data from the Carpathian range, Romania. *Journal of Hydrology*. doi: 10.1016/j.jhydrol.2010.07.019.

First received 17 November 2015; accepted in revised form 9 September 2016. Available online 29 November 2016